Supplementary Figures

List of Supplementary Figures

Figures	Description
Supplementary Figure 1	Overview of intron retention in mice.
Supplementary Figure 2	Expression correlation between retained introns and their parental genes in humans and mice.
Supplementary Figure 3	Sequence conservation of retained introns between human and mouse using the *SRSF6* gene as an example
Supplementary Figure 4	Validation of retained introns in humans using custom Nanostring chip.
Supplementary Figure 5	Validation of retained introns in mice using custom Nanostring chip.
Supplementary Figure 6	RT-PCR validation of 21 retained introns in mice.
Supplementary Figure 7	Number of retained intron-specific peptides detected using mass spectrometry
Supplementary Figure 8	Amino acids sequence of the intron-retaining protein isoform of *PLEC* and EIF2D in humans.
Supplementary Figure 9	Smear plot of differential expressed retained introns (DEIs) in human brain (blue).
Supplementary Figure 10	The distributions of absolute values of edge weight (regression coefficients, denoted as β) of SPIRON for human and mouse, respectively.
Supplementary Figure 11	In humans, the observation that introns appear to be regulated by a major splicing gene is robust to changes of modeling approaches. Here, it is illustrated by using a different approach, called Elastic Net (EN), to build AD-specific SPIRONs. For EN, its parameter alpha was set to 0.2 and 0.5, respectively.
Supplementary Figure 12	In mice, the observation that introns appear to be regulated by a major splicing gene is robust to changes of modeling approaches. Here, it is illustrated by using a different approach, called Elastic Net (EN), to build AD-specific SPIRON. For EN, its parameter alpha was set to 0.2 and 0.5, respectively.
Supplementary Figure 13	Comparison of the regulatory patterns of splicing factors between human and mice in the control samples.
Supplementary Figure 14	Comparison of the degree (left panel) and average weight (right panel) of each splicing factor between the control and AD-specific SPIRONs.
Supplementary Figure 15	The correlation of the eigengene (PC1 stands for the first principal component) of the SNRPF, PCF11, HNRNPH1, PTBP1 modules with Braak score.

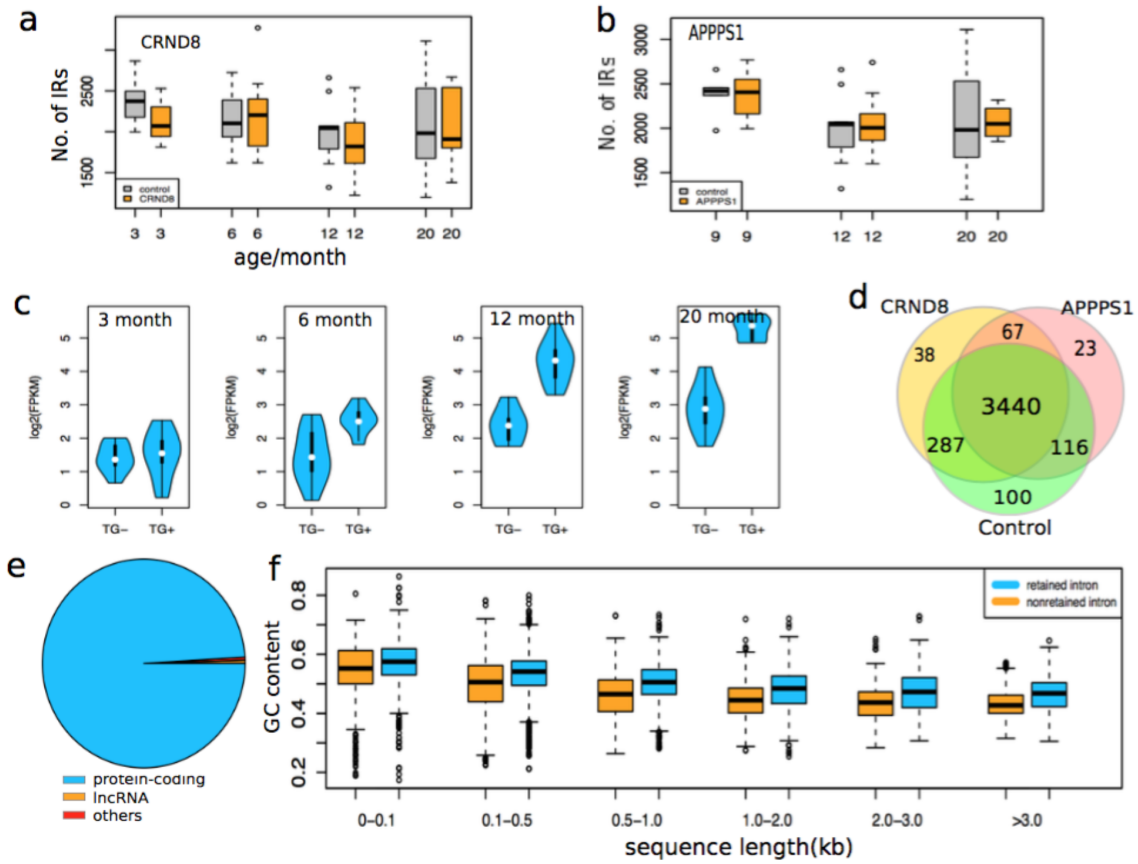

Supplementary Figure 1. Overview of intron retention in mice. **a** and **b** show the number of **i**ntron retentions in CRND8 and APPPS1 transgenic mice, respectively. **c**, expression comparison of the intron (Chr17:34734207-34734364) of *C4b* gene between transgenic and control mice across ages. **d**, the Venn diagram of IR in control, CRND8 and APPPS1 mice. **e**, the biotype distribution of parent genes of retained introns. **f,** GC content comparison between retained and non-retained introns grouped by length.

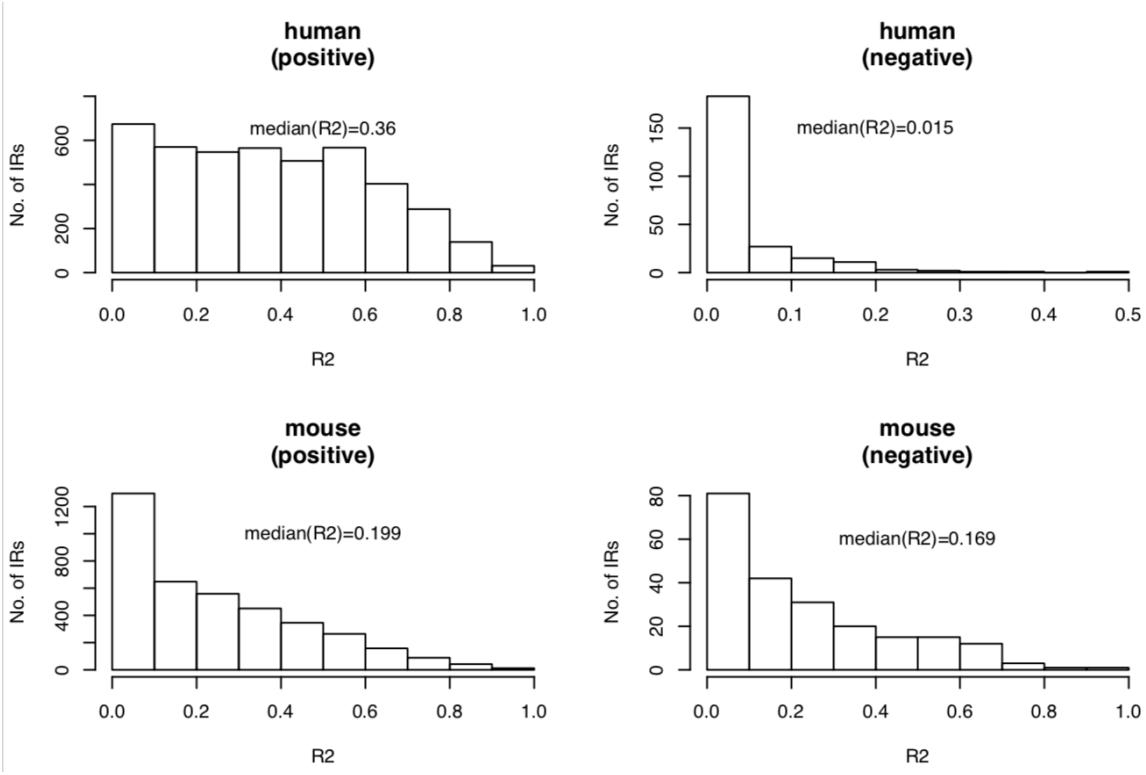

Supplementary Figure 2. Expression correlation between retained introns and their parental genes in humans and mice. For both humans and mice, the distribution of the correlation in terms of R^2 is shown for the posively and negatively correlated intron-gene pairs, respectively.

Supplementary Figure 3. Sequence conservation of retained introns between human and mouse using the *SRSF6* gene as an example. The intron of this gene in human (chr20:43459420-43459770, ENSG00000124193) was blasted against the intron in mouse homologue (chr2:162933082-16293325, ENSMUSG00000016921). The sequence identity is 93% with e-value 6.0e-144; this intron is highly conserved between human and mouse.

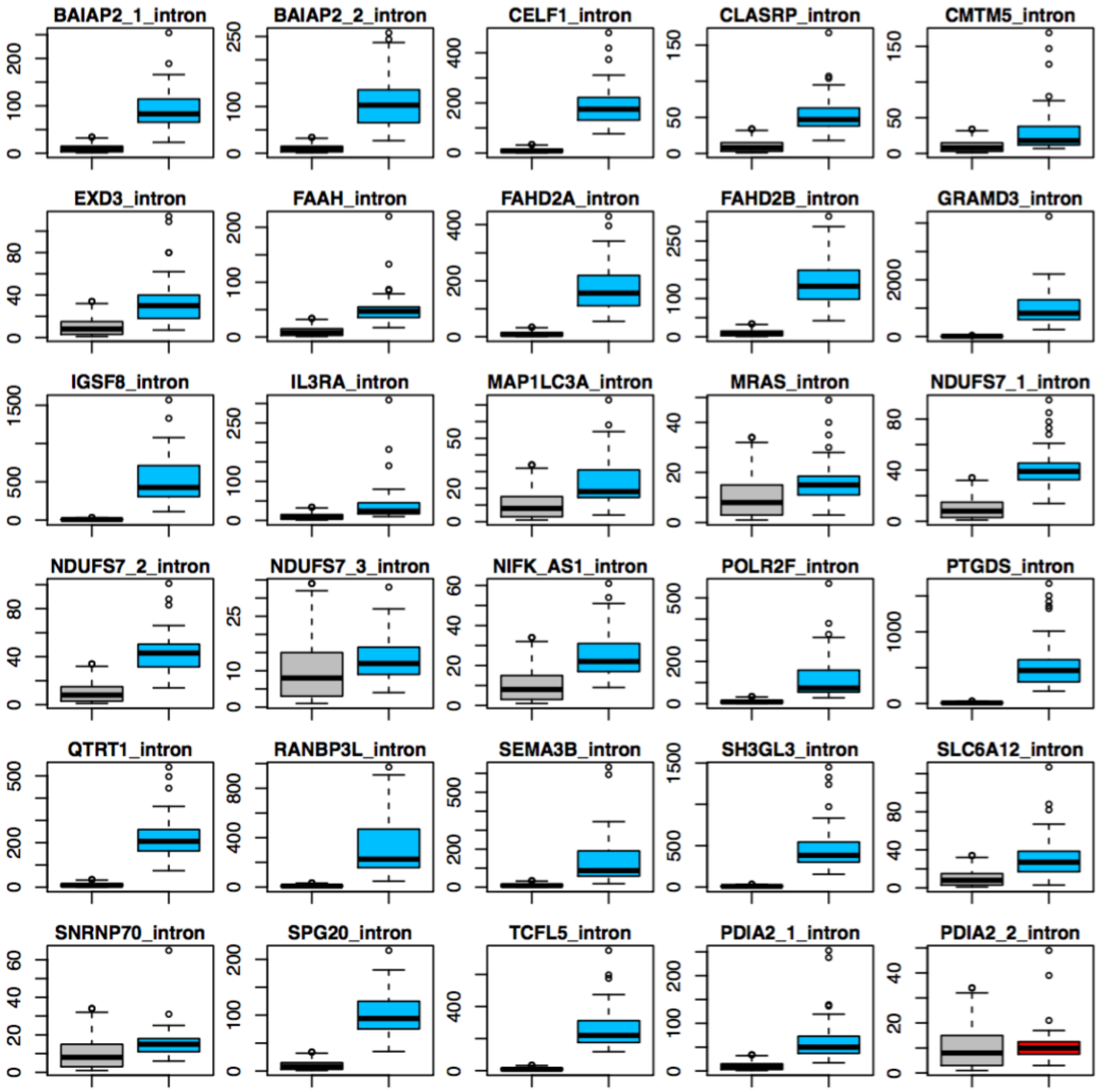

Supplementary Figure 4. Validation of retained introns in humans using custom Nanostring chip. Based on Mann Whitney U test and Benjamin-Hochberg correction, it was found that 29 out of the 30 tested introns showed significantly higher expression compared to negative control probes (adjusted p value < 0.05). The non-significant intron is PDIA2_2_intron (boxplot in red color). Gray color boxplots are for negative control probes. Blue or red boxplots are for retained introns.

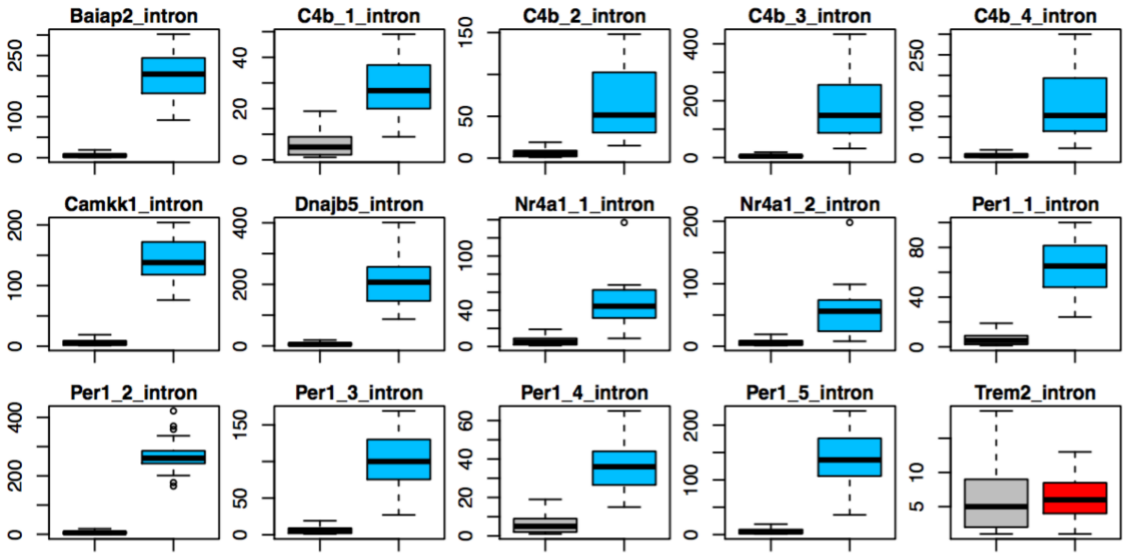

Supplementary Figure 5. Validation of retained introns in mice using custom Nanostring chip. Based on Mann Whitney U test and Benjamin-Hochberg correction, it was found that 14 out of the 15 tested introns showed significantly higher expression compared to negative control probes (adjusted p value < 0.05). The non-significant intron is Trem2_intron (boxplot in red color). Gray color boxplots are for negative control probes. Blue or red boxplots are for retained introns.

Gene	Introns and RT-PCR validation
Baiap2	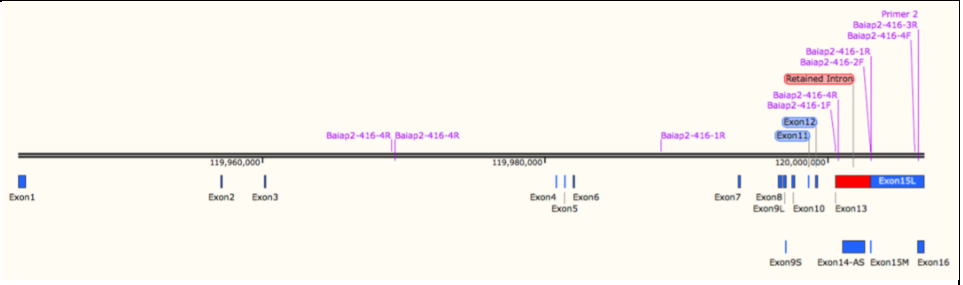 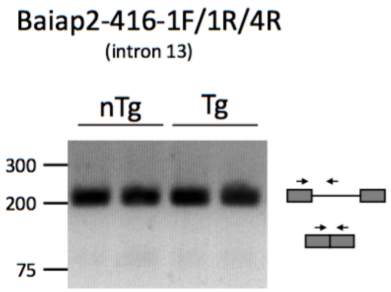
C4b	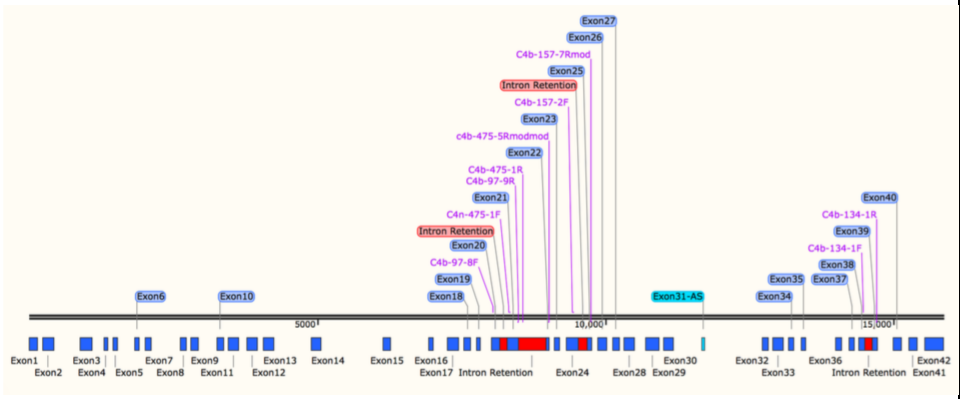 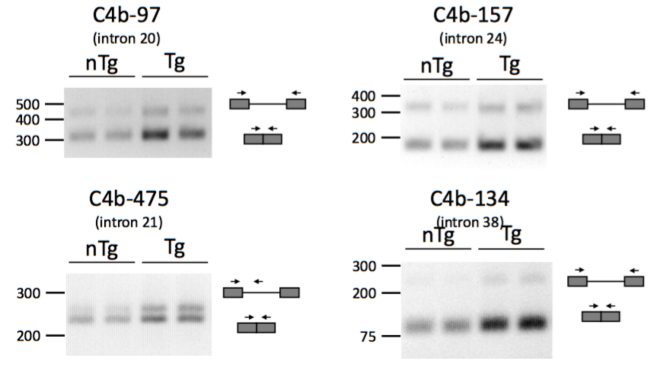

Dnajb5	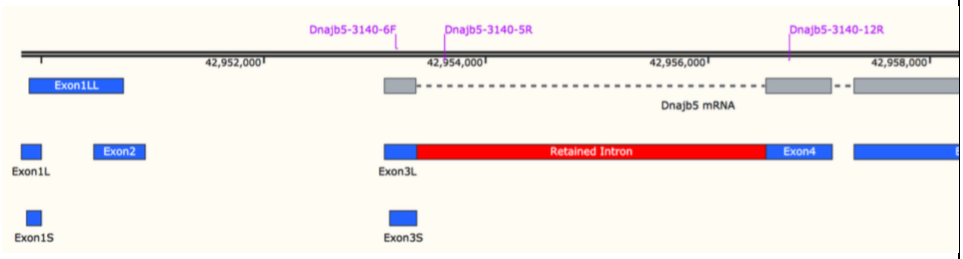 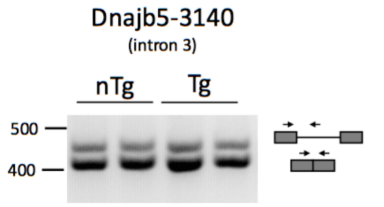
Trem2	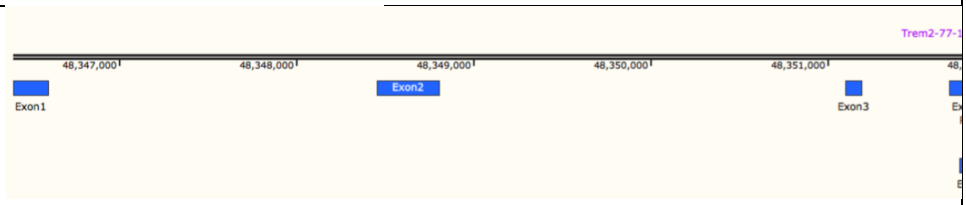 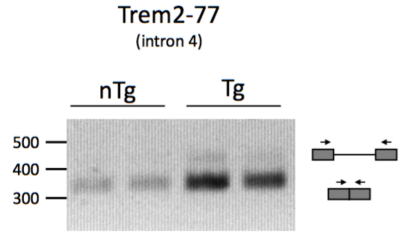
Camkk1	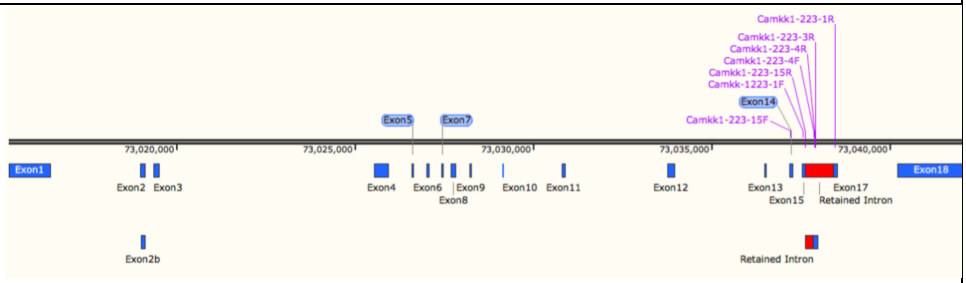 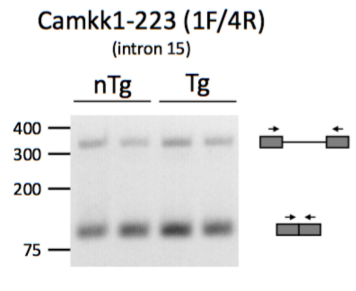 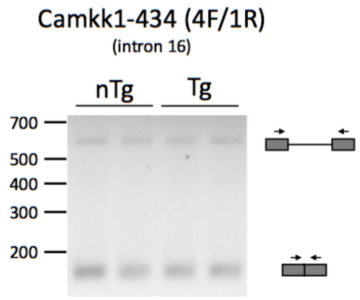

Nr4a1	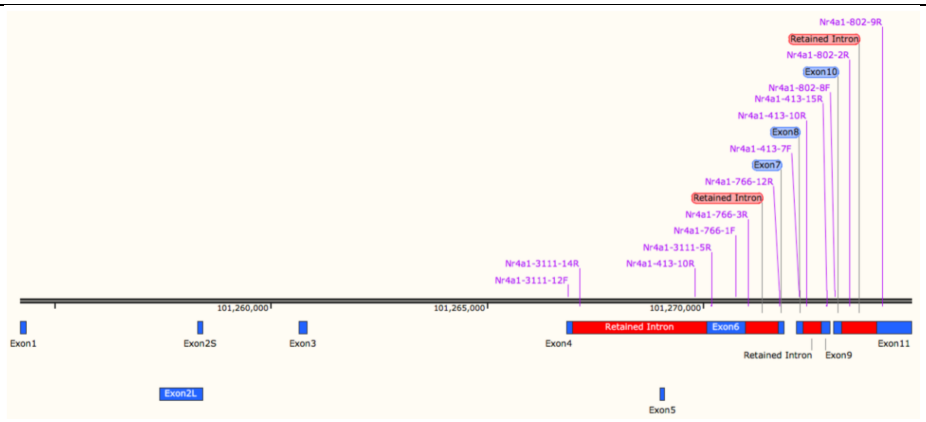 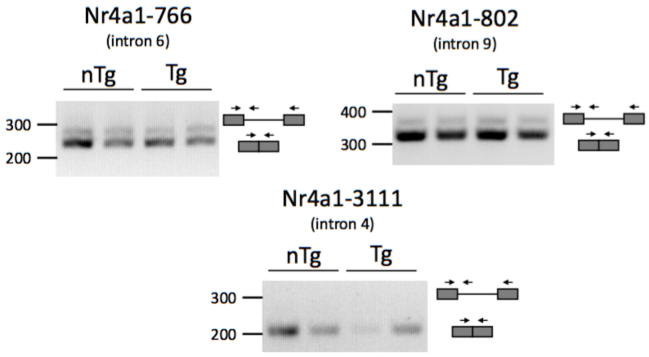
Per1	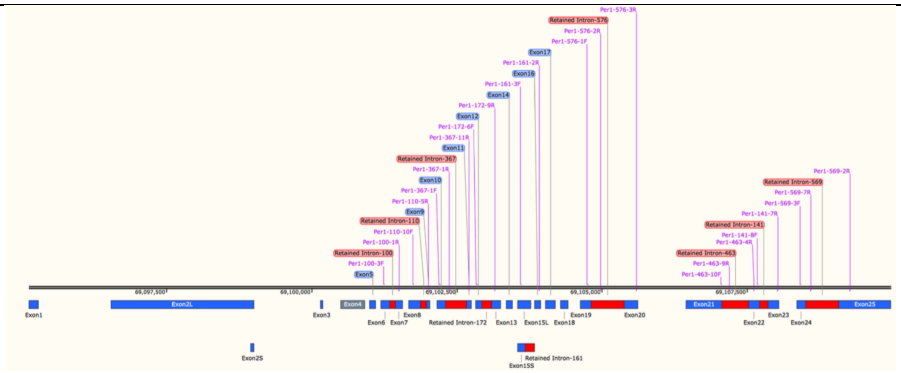 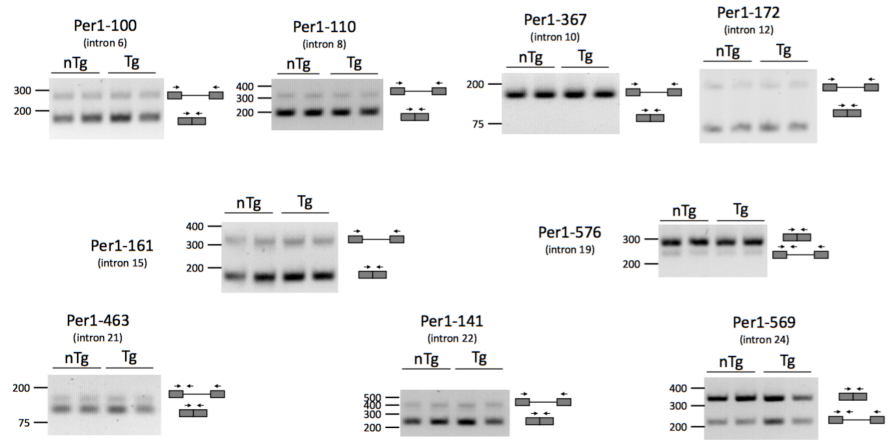

Per2	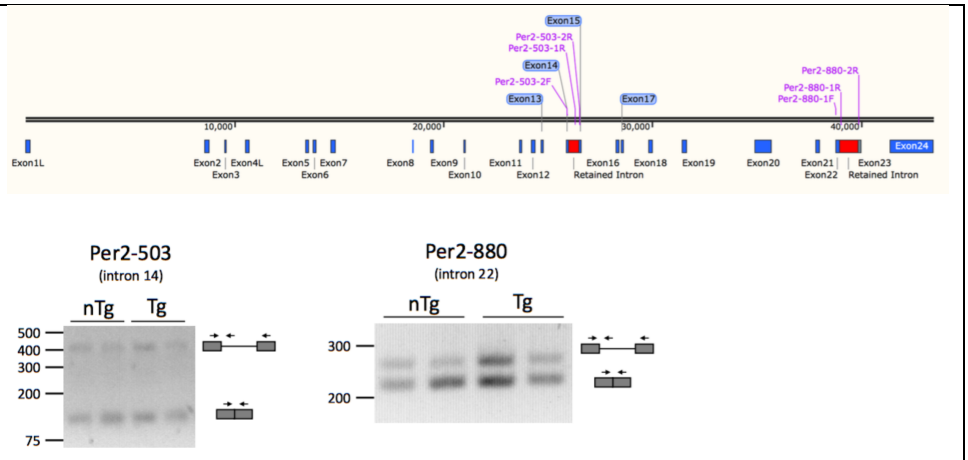

Supplementary Figure 6. RT-PCR validation of 21 retained introns in mice.

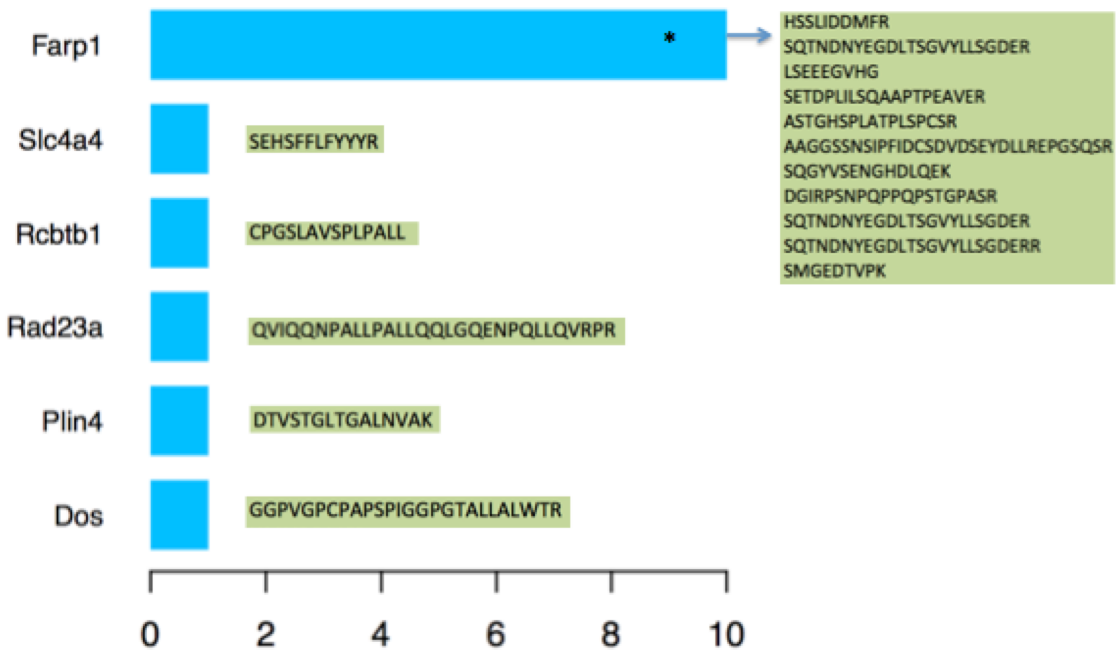

Supplementary Figure 7. Number of retained intron-specific peptides detected using mass spectrometry (*: number of unique non-nested peptides). Amino acid residue sequences of peptides are also given. The uniqueness of these peptides were validated using nextProt ‘peptide uniqueness checker’ as well as Peptideatlas.

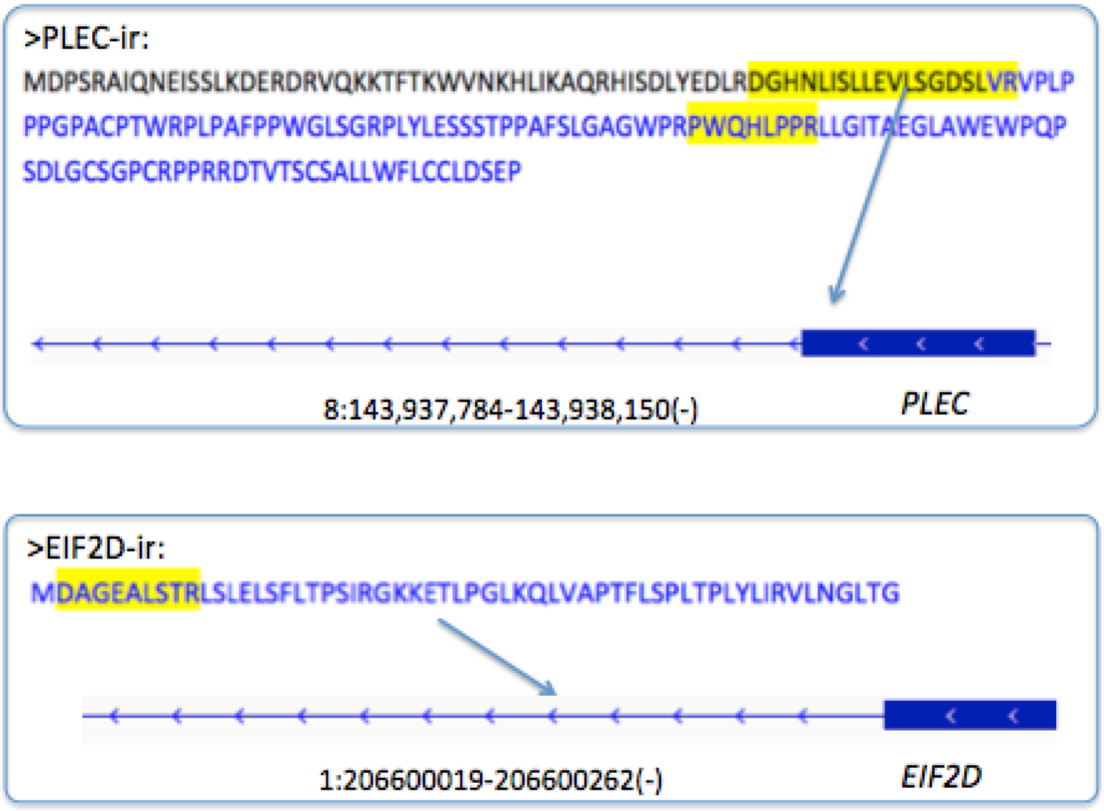

Supplementary Figure 8. Amino acids sequence of the intron-retaining protein isoform of *PLEC* and EIF2D in humans. Highlighted in yellow are two peptides with mass spectral evidence (FDR<0.01 at both peptide and protein level).

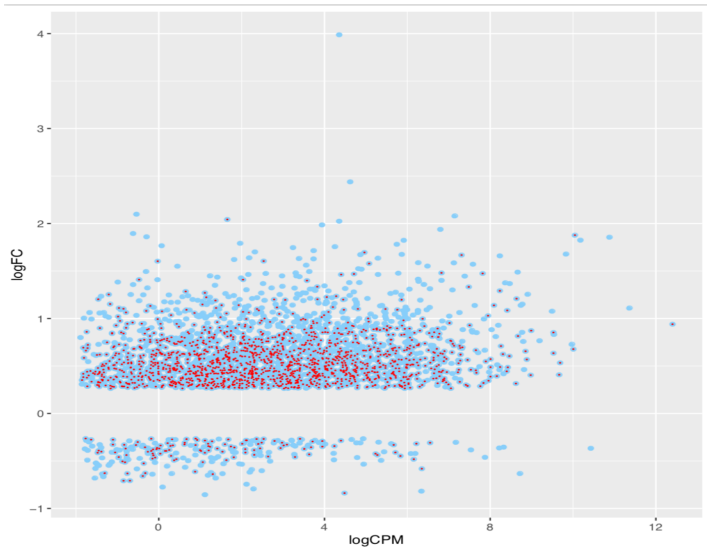

Supplementary Figure 9. Smear plot of differential expressed retained introns (DEIs) in human brain (blue). A red dot indicates that the parental gene of the intron is not differentially expressed based on exon expression.

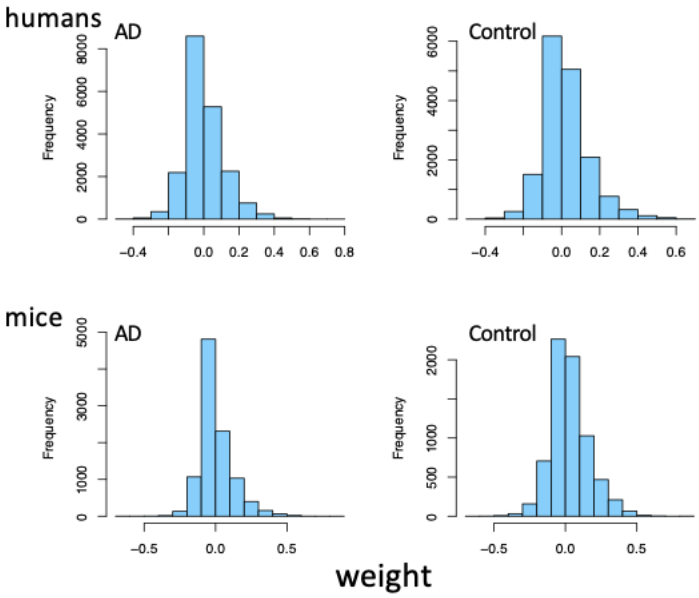

Supplementary Figure 10. The distributions of the edge weight (regression coefficients, denoted as β) of the SPIRON for humans and mice, respectively. The edge weight of the full SPIRON is analyzed here.

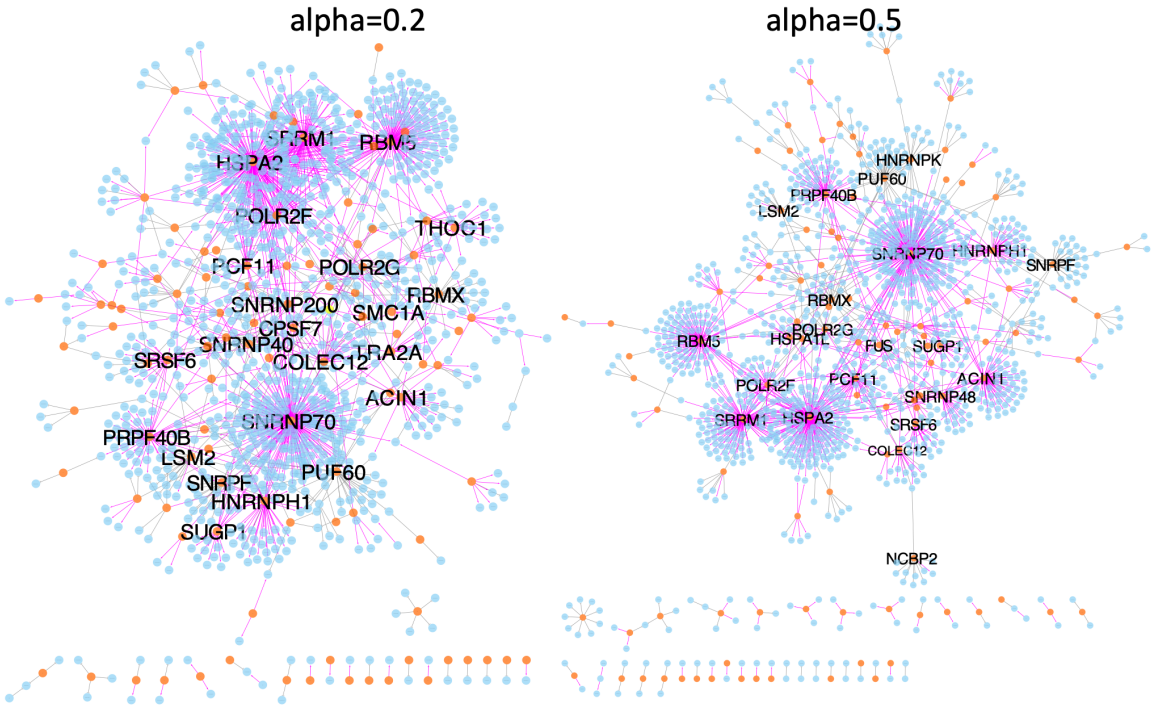

Supplementary Figure 11. In humans, the observation that introns appear to be regulated by a major splicing gene is robust to changes of modeling approaches. Here, it is illustrated by using a different approach, called Elastic Net (EN), to build AD-specific SPIRONs. For EN, its parameter alpha was set to 0.2 and 0.5, respectively.

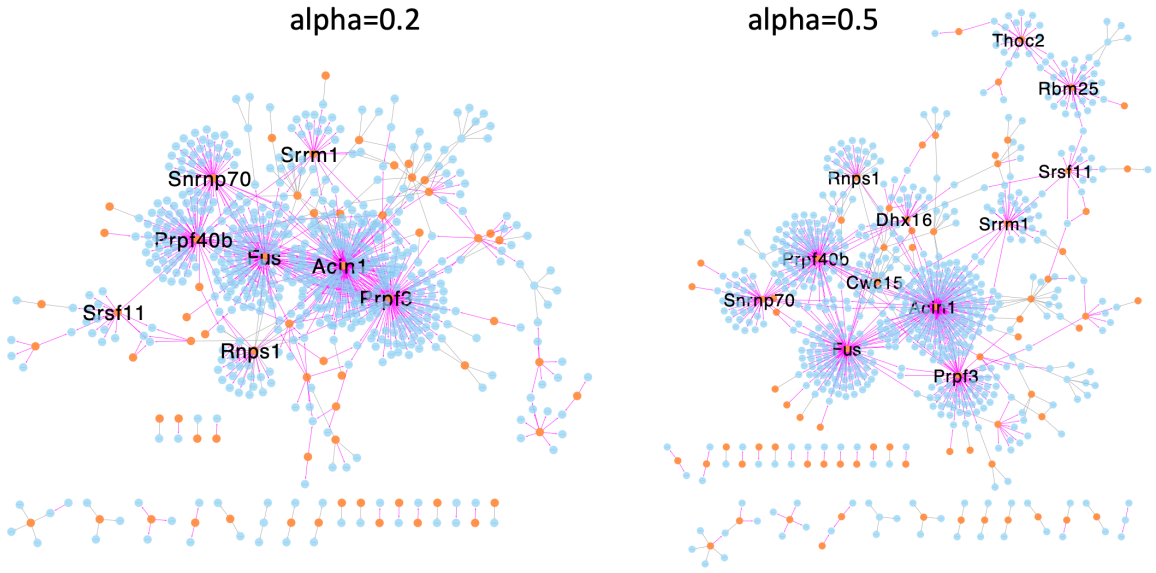

Supplementary Figure 12. In mice, the observation that introns appear to be regulated by a major splicing gene is robust to changes of modeling approaches. Here, it is illustrated by using a different approach, called Elastic Net (EN), to build AD-specific SPIRON. For EN, its parameter alpha was set to 0.2 and 0.5, respectively.

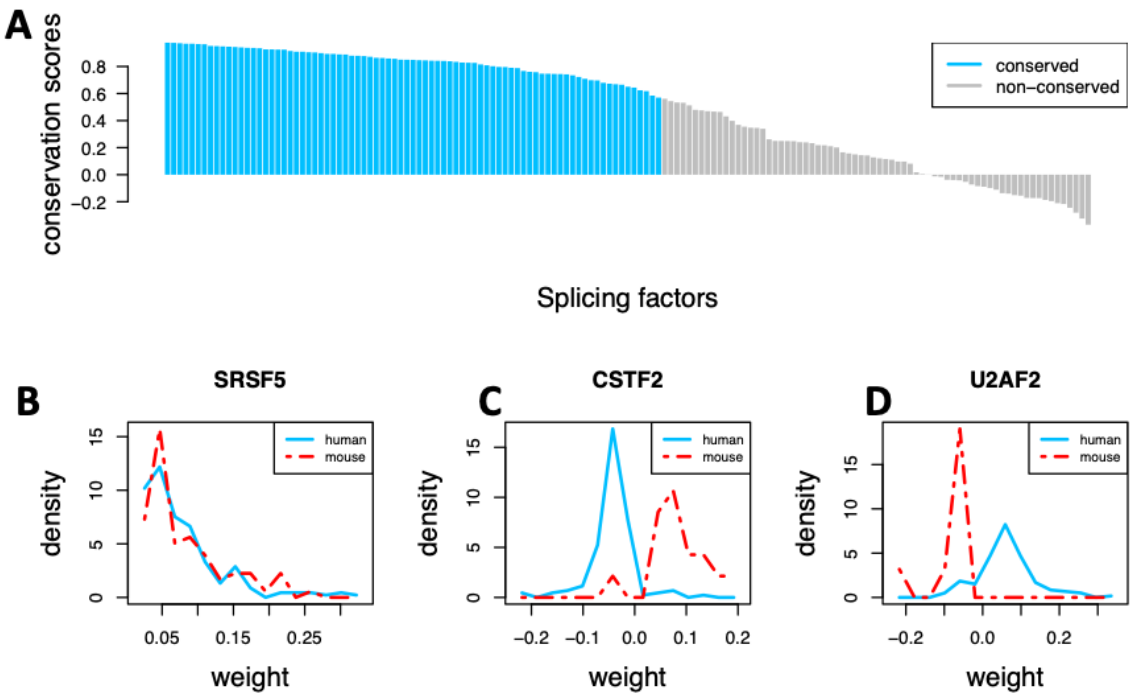

Supplementary Figure 13. Comparison of the regulatory patterns of splicing factors between human and mice in the control samples. (**A**) For each splicing factor, we computed a conservation score (ranging from -1 to 1) between the human and mouse SPIRON network (**Materials and methods**). Most splicing factors show conserved regulatory patterns (FDR<0.01). (**B**) Illustration of conserved regulatory patterns with *SRSF5*. (**C**) Illustration of opposite regulatory directions of splicing factors between human and mouse with *CSTF2,* which negatively regulates retained introns in human but positively in mouse. (**D**) In contrast, *U2AF2* positively correlates retained introns in human but negatively in mouse. Note: weight is the edge weight between splicing factors and introns in the SPIRON network.

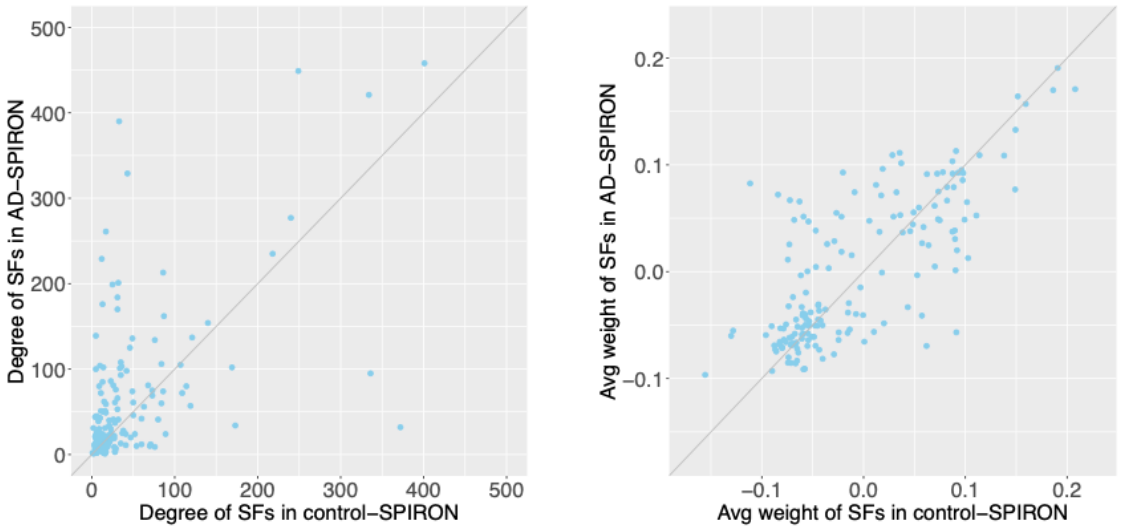

Supplementary Figure 14. Comparison of the degree (left panel) and average weight (right panel) of each splicing factor between the control and AD-specific SPIRONs.

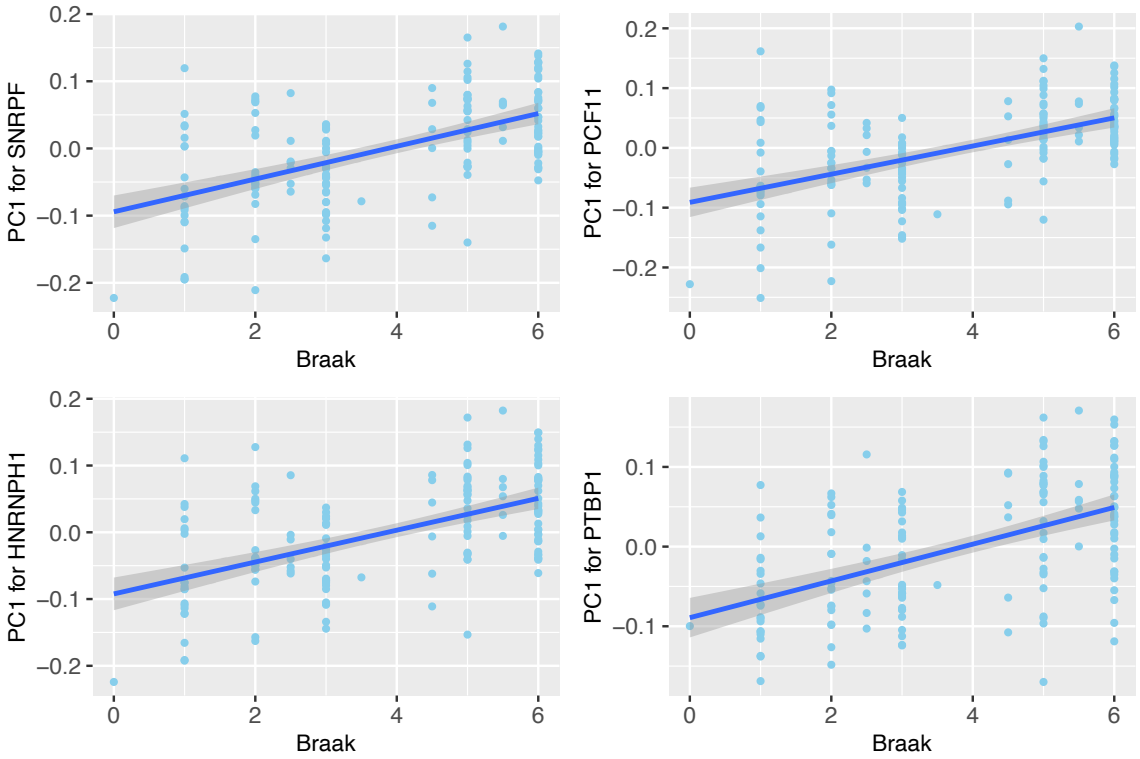

Supplementary Figure 15. The correlation of the eigengene (PC1 stands for the first principal component) of the SNRPF, PCF11, HNRNPH1, PTBP1 modules with Braak score. The Spearman correlation of the four genes with Braak score are 0.524, 0.524, 0.519 and 0.515, respectively. The FDR of the four correlations are smaller than 0.0001.